

# Identifying the electronic character and role of the Mn states in the valence band of (Ga,Mn)As

J. Fujii<sup>1</sup>, B. R. Salles<sup>1</sup>, M. Sperl<sup>2</sup>, S. Ueda<sup>3</sup>, M. Kobata<sup>3</sup>, K. Kobayashi<sup>3,4,5</sup>, A. Ashita<sup>3</sup>, M. Sorelli<sup>1</sup>, M. Utsumi<sup>2</sup>, & S. Fadley<sup>6</sup>, J. Minar<sup>10</sup>, J. Braun<sup>10</sup>, J. Bert<sup>10</sup>, O. I. Marzari<sup>11</sup>, S. F. Bruneau<sup>11</sup>, M. S. S. Feher<sup>13</sup>, S. Suardi<sup>13</sup>, S. Strydom<sup>13</sup>, J. O. Andersen<sup>14</sup>, & M. Baerlin<sup>15</sup>, A. D. Edwards<sup>19</sup>

<sup>1</sup>*Istituto Officina dei Materiali (IOM)-CNR, Laboratorio TASC, in Area Science Park, S.S.14, Km 163.5, I-34149 Trieste, Italy*

<sup>2</sup>*Institut für Experimentelle Physik, Universität Regensburg, D-93040 Regensburg, Germany*

<sup>3</sup>*NIMS beamline Station at Spring-8, National Institute for Materials Science, Sayo, Hyogo 679-5148, Japan*

<sup>4</sup>*Japan Atomic Energy Agency, Sayo, Hyogo 679-5148, Japan*

<sup>5</sup>*Hiroshima Synchrotron Radiation Center, Hiroshima University, 2-313 Kagamiyama, Higashi-Hiroshima, Japan*

<sup>6</sup>*Advanced Electric Materials Center, National Institute for Materials Science, 1-1 Namiki, Tsukuba, Ibaraki 305-0044, Japan*

<sup>7</sup>*Department of Physics, University of California, Davis, California 95616, USA*

<sup>8</sup>*Material Sciences Division, Lawrence Berkeley National Laboratory, Berkeley, California 94720, USA*

<sup>9</sup>*Stanford Institute for Materials and Energy Sciences, SLAC National Accelerator Laboratory, Menlo Park, California 94025, USA*

<sup>10</sup>*Department of Chemistry, Ludwig Maximilian University, D-81377 Munich, Germany*

<sup>11</sup>*Department of Physics and Astronomy, Uppsala University, Box 516, SE-75120, Uppsala, Sweden*

<sup>12</sup>*Institute for Solid State Physics, Vienna University of Technology, 1040 Vienna, Austria*

<sup>13</sup>*Max Planck Institute for Chemical Physics of Solids, 01187 Dresden, Germany*

<sup>14</sup>*Japan Synchrotron Radiation Research Institute, SPring-8, Hyogo 679-5198, Japan*

<sup>15</sup>*Diamond Light Source, Chilton, Didcot, Oxfordshire OX11 0DE, United Kingdom*

## ABSTRACT

We report high-resolution hard x-ray photoemission spectroscopy results on (Ga,Mn)As. As a function of Mn doping, supported by theoretical calculations, we observe the emergence of a band at 13 eV below the valence band. The electronic character of the states near the top of the valence band of (Ga,Mn)As is temperature dependent. We observe the emergence of a band at 13 eV below the valence band of (Ga,Mn)As.

Understanding the electronic and magnetic properties of diluted magnetic semiconductors is important for the development of materials for spintronics. In this paper, we report the results of high-resolution photoemission spectroscopy (HRPES) measurements on (Ga,Mn)As. The results show the emergence of a band at 13 eV below the valence band of (Ga,Mn)As, which is identified as the Mn d-orbitals. The electronic character of the states near the top of the valence band of (Ga,Mn)As is temperature dependent. We observe the emergence of a band at 13 eV below the valence band of (Ga,Mn)As.

de2ade, a-d 2arrier; ! ediated ?erro ! a6-etis ! is u-doubtedly o-e o? the ! ost dis2ussed  
 issues i- 1 MS resear2h B1;"C. \$he 2ase o? the =+a,M->)s 7ale-2e ba-d is prototypi2alD  
 : hether the states -ear the Fer ! i le7el,  $E_F$ , are best des2ribed i- ter ! s o? dispersi7e  
 states ?ully ! er6ed @ith the +a) s 7ale-2e ba-d or i? these states preser7e the 2hara2ter o?  
 a- i ! purity ba-d, has bee- a 2e-tral issue o? i-te-se a2ti7ity i- solid;state s2ie-2e,  
 holdi-6 i ! porta-t ra ! i?i2atio-s ?or the de7elop ! e-t o? ?uture spi-tro-i2s ! aterials B3;  
 "C. Both des2riptio-s sta-d o- 7arious e<peri ! e-tal a-d theoretial ar6u ! e-ts that ?a7or  
 o-e or the other o? these t@o 7isio-s B5; ,C, a-d ! ore re2e-tly u-i?ied pi2tures, i-7ol7i-6  
 both ideas, ha7e bee- prese-ted B1E;13C. Fo-etheless, the 2rosso7er re6i ! e bet@ee-  
 i ! purity states at lo@ dopi-6 a-d truly e<te-ded states at hi6h dopi-6, @ith possibly  
 Blo2h;li4e 2hara2teristi2s, i.e., the esse-2e o? ho@ ?erro ! a6-etis ! is established i-  
 =+a,M->)s, is ?ar ?ro ! a u-i?ied a-d 2lear des2riptio-. Su2h a des2riptio- is i-ti ! ately  
 li-4ed to a ?urther 2e-tral Guestio-D ho@ i ! porta-t is lo2ali%atio- 7s. hybrid%atio- o?  
 2arriers i- the 7i2i-ity o?  $E_F$  as a ?u-2tio- o? dopi-6H \$heoretial ! odeli-6 has so ?ar  
 o-ly o??ered a- i-2o-2lusi7e 2o-tributio- to this issue, si-2e disorder a-d stro-6  
 ele2tro-i2 2orrelatio-s re-der realisti2 ele2tro-i2 stru2ture 2al2ulatio-s di??i2ult to  
 per?or ! . 3- the e<peri ! e-tal ?ro-t, ?ull 2o-trol o? the syste ! is hard to a2hie7e a-d o-ly  
 a li ! ited -u ! ber o? dire2t ! easure ! e-ts o? the 7ale-2e ba-d ele2tro-i2 stru2ture o?  
 =+aM->)s ha7e bee- reported B14,15C . \$he -eed to o7er2o ! e the solubility li ! it to  
 obtai- stable 2o-ditio-s ?or ?erro ! a6-eti2 order, thus i ! posi-6 o??;eGuilibriu ! 6ro@th  
 2o-ditio-s, stro-6ly i-?lue-2es the ho ! o6e-eity o? =+a,M->)s. Reliable e<peri ! e-tal  
 e7ide-2e e<ists, e.6., ?or a depletio- %o-e -ear the i-ter?a2e i- de7i2e;li4e stru2tures that  
 are respo-sible ?or dra ! ati2 2ha-6es i- the hole;de-sity pro?ile, a22o ! pa-ied by a stro-6

reduction of the temperature,  $T \approx 10^3$  K. Moreover, the presence of both substitutional and interstitial double-donor sites in purities at high Mn concentrations, in addition to their opposite contributions to the magnetic properties, leads to a pronounced difference between the electrical properties at  $10^3$  K.

In the present work, we exploit the hard X-ray photoemission spectroscopy (XPS), corresponding to a severely suppressed  $1s$  contribution at  $10^3$  K, where the doublet structure of the band and core level, in addition to the temperature dependence of the magnetic properties, allows a direct determination of the band density of states near  $E_F$  as a function of Mn doping. Supported by theoretical calculations, we observe that, although the band structure is substantially modified by Mn doping, a clear  $1s$  feature with Mn character is present, starting at a Mn doping level as low as  $1\%$ , where the Fermi level is located well above the band host band top, and where the delocalized character of the Mn states has a direct relation with the magnetic properties.

We have studied three different  $1s$  features in Mn  $1s$ ,  $5s$ , and  $13s$  doping, in order to investigate the nature of the doublet structure observed by the XPS measurements. Samples grown by molecular beam epitaxy on  $\text{Si}$  substrates, under low temperature growth conditions, were measured at different temperatures, from  $10$  K to  $300$  K, using a synchrotron radiation source with a resolution of  $0.1$  eV. The overall energy resolution is  $0.1$  eV, as verified by the spectra of the  $1s$  band at the Fermi level for a polycrystalline sample in the electrical and optical measurements.

$\rightarrow$  s spectra. The energy levels are measured from the Fermi level  $E_F$  as indicated in Fig. 1. Further details of the photoemission spectroscopy procedure and calculations are given in Ref. 1.

In Fig. 1 the photoemission spectroscopy spectra of pure  $\text{Mg}$  and  $\text{Mg}_{1-x}\text{Al}_x$  alloys, with increasing Al content, are compared with the theoretical curves based on the band structure calculations. For the sake of comparison, the  $\text{Mg}$  spectra have been aligned to the  $\text{Mg}$  spectra using the band structure calculation. The energy levels are based on the band structure calculation of density functional theory (DFT), the self-consistent potential approach to describe the presence of the  $\text{Mg}$  dopant, and density functional theory (DFT) as implemented with the multiple scattering method for  $\text{Mg}_{1-x}\text{Al}_x$ . The calculations agree qualitatively with the experimental data over a wide energy range. The  $4s$  states are located at  $\sim 1\text{ eV}$  below  $E_F$  and their energy hybridization with the  $\text{Mg}$   $3d$  states is small as they are well separated in energy from  $E_F$ , the  $\text{Mg}$   $3d$  states of  $e_g$  symmetry hybridize mainly with the  $4p$  and  $4s$  states. Instead, the  $\text{Mg}$   $3d$  states of  $t_{2g}$  symmetry exhibit a more significant hybridization just below  $E_F$ .

In Fig. 1, the high-resolution spectra measured in the vicinity of  $E_F$  are displayed for pure  $\text{Mg}$ ,  $1\text{A}$  and  $13\text{A}$   $\text{Mg}_{1-x}\text{Al}_x$  alloys. The dashed lines are the derivative spectra, with the pure  $\text{Mg}$  spectrum subtracted from the  $13\text{A}$  and  $1\text{A}$   $\text{Mg}_{1-x}\text{Al}_x$  spectra and grey, respectively, in order to highlight the multiplet  $\text{Mg}$  contribution. In Fig. 1, the

calculated difference spectra,  $\pm$  as subtracted from  $\pm$   $M \rightarrow$  states, are presented for the  
 81) and 1MF\$ calculations of violet and green features, respectively. Both the  
 experimental and calculated spectra show a pronounced feature caused by  $M-d$  states, arising  
 from a mixture of  $d$  states, localized around the  $d$  purity, and  $M-d$  states.  
 The strong hybridization redistributes the spectral weight of the  $M-d$  states over a wide  
 energy range all the way up to  $E_F$ . The evolution as a function of doping shows a  
 decrease in intensity of the  $M-d$  band. In addition, the intensity of our resolution, or shift of the  $M-d$   
 band is observed. The  $M-d$  spectral weight is peaked at 0.3 eV below  $E_F$ , in  
 agreement with previous surveys of photoemission data [14], and recent hard x-ray  
 angle-resolved photoemission spectroscopy [11]. It is important to emphasize that the  $M-d$ -related  
 features near  $E_F$ , although significantly smaller, is also observed in the energy resolution.  
 The diluted nature of  $M-d$  in the host system is illustrated by the spectroscopy  
 of the difference spectra in Fig. 1. The  $M-d$  states in  $\pm$   $M \rightarrow$  states retain their  
 characteristic shape because the doping value increases up to a  $M-d$  doping  
 high as 13A, a value scarcely considered to display metallic behavior, whereas for  $M-d$   
 a truly metallic system, one obtains a clear Fermi level, or are cluster-related features found  
 in zero-field photoemission spectroscopy and x-ray absorption spectroscopy [1, C].

In addition, ascertained the nature and evolution of the  $M-d$  states in the vicinity of  $E_F$ ,  
 we further address their role in the electronic properties of the  $\pm$   $M \rightarrow$  system by  
 means of zero-field studies. In previous work, zero-field x-ray spectroscopy  
 was able to demonstrate, via comparison with  $d$ -derived  $d$  purity model [10], that  
 calculations, the importance of hybridization is. Localization of  $d$ -electrons in  $\pm$   $M \rightarrow$  states

B25,2"CR to su2h ! easure! e-ts, @e ha7e -o@ added ! a6-eti2 se-siti7ity by usi-6  
 2ir2ularly polari%ed <;rays, thus e-abli-6 M&1;#/S. Fi6ure 2 sho@s the 2ore;le7el  
 . ) \*# / S =hv M ', 4E eK> ?or a 13A M- doped +a) s sa! ple i- the ?erro ! a6-eti2 state  
 =belo@ its &urie te ! perature,  $T_{\& M (E K>$ , a-d 2o ! pared to ! odel 2al2ulatio-s. Fi6ure  
 2-a> sho@s a sur7ey spe2tru ! that lo2ates the M- 2p doublet o? i-terest, a-d ide-ti?ies the  
 @ell; a-d poorly;s2ree-ed ?eatures a-d ! ultiplet stru2ture o? the  $2p_{3s2}$  a-d  $2p_{1s2}$  2ore  
 le7els, i- a6ree ! e-t @ith pre7ious results B25,2"C. Fi6ure 2=b> sho@s the M&1 ?or the  
 ?ull M- 2p regio-, @ith a 7ery lar6e ! a6-eti2 asy ! ! etry o? 013A. 0t has pre7iously bee-  
 -oted that the li-e shape o? the M- 2p 2ore le7el does -ot 2ha-6e @hile 7aryi-6 the M-  
 2o-2e-ratio- ?ro! 1A to 13A, @hi2h is stro-6 e7ide-2e a6ai-st a- i ! porta-t  
 2o-tributio- o? i-terstitial M- ato ! s i- our bul4;se-siti7e spe2tra B25C. \$he 2al2ulatio-s  
 i- Fi6. 2=2>, usi-6 the )0M ! odel B1,C, sho@s that the  $2p_{3s2}$  stru2ture 2o-tai-s a @ell;  
 s2ree-ed pea4 at the hi6h 4i-eti2 e-er6y =lo@ B /> side a-d a poorly;s2ree-ed pea4 at 1;2  
 eK lo@er 4i-eti2 e-er6y =hi6her B />, @ith opposite di2hrois ! B25,2"C. \$he @ell;  
 s2ree-ed pea4 is ?ou-d to ha7e ! ai-ly  $2p^5 3d^h^2$  2hara2ter, @hile the poorly s2ree-ed pea4  
 has ! ai-ly  $2p^5 3d^5 h$  2hara2ter, @here  $h$  de-otes a hole state. 0- the 6rou-d state, the  $3d^5 h$   
 state is pi--ed to  $E_F$ , a-d it is the  $3d^h^2$  state @hi2h is pulled do@- i- e-er6y i- the ?i-al  
 state due to the 2p 2ore;hole pote-tial B25C. 0- the 2al2ulatio-, the lo2al 6rou-d state  
 properties are pri ! arily re?le2ted by t@o para ! eters. \$he tra-s?er i-te6ral,  $V$ , respo-sible  
 ?or the hybridi%atio- = ! i<i-6> a-d the o-;site 3d ele2tro-;repulsio- e-er6y,  $U$ , i.e., the  
 . ubbard  $U$ . For s ! all  $UV$  the ele2tro-s are delo2ali%ed, @hereas ?or lar6e  $UV$  the  
 ele2tro-s are lo2ali%ed o- the ato ! i2 sites. \$he e<peri ! e-tal M&1 o? the . ) \*# / S  
 a6rees 7ery @ell @ith the 2al2ulated spe2tra ?or a hybridi%atio- para ! eter  $2.E \leq K \leq 2.5$

eK. It is important to emphasize that the most interesting feature, at the energy  
 resolution corresponding to the leaded ellipsoidal peak, is linked to the most  
 delocalized electronic character, a feature already put forward by the results of  
 Brogliato *et al.* [2] and Gooding *et al.* [3].

In addition, the role played by the hybridization of the  $M-3d$   
 states is obtained from the temperature dependence of the carrier  
 concentration in a heavily doped semiconductor, such as  $\text{GaMnAs}$ , does not change  
 significantly with temperature [2], a sign of the more localized nature of the  
 spectral weight. The temperature is associated with a change in the  
 delocalized electronic states. The results are shown in Fig. 3 for the  $2p$   
 more localized  $M-3d$ , and compared to the  $7d$  band. While the  $2p$  peak  
 shifts from  $E_F$  to higher  $B$  with temperature, the measured  $7d$   
 band shift is less than half of this value. This temperature dependence implies a  
 reduced  $M-3d$  hybridization, and hence a more electronic hopping  
 error [2]. Moreover, the low  $B$  feature of the  $M-2p_{3/2}$  more localized  
 associated with the more delocalized  $d^5h^2$  states shifts with temperature by 0.35 eV,  
 whereas the shift of the broad component at higher  $B$  corresponding to the more  
 localized  $d^5h$  states is detected. This observation implies that the  $2p_{3/2}$  is  
 associated exclusively to the more hybridized  $M-3d$  states, while the localized  $M-  
 d^5h$  states, in the vicinity of  $E_F$ , do not participate in the  $2p_{3/2}$  process. Further  
 observation of this picture shows that the calculated  $M-3d$  in Fig. 2b, where the  
 energy separation between the sharp feature peak and broad positive peak in the  $M-  
 2p_{3/2}$  increases with  $V_R$  this again implies a more electronic  $2p_{3/2}$  due to delocalized

electro-s. Therefore, the observed B / shifts are not due to surface effects. It is important to understand that the  $\epsilon$  and the  $\epsilon_2$  are perpendicular prior to introducing the samples into the furnace. The surface states and results in a complete upturn of the Fermi level B1, C.

The physical scenario for our two biased observations and calculations is presented in Fig. 4. The  $\epsilon$  band is substantially modified by the introduction of M atoms, especially for dopings as low as 1%. The largest modification of the  $\epsilon$  band is found over the  $2;4$  eV B/. For all M dopings studied, over the  $1;13$  eV of the measured  $\epsilon$  band, the energy separation from the top of the  $\epsilon$  band states to  $E_F$  is in the order of  $5E$  eV, after taking into account the experimental energy resolution, resolution with the Fermi level, and possible recombination effects B1, C. The resolution as a function of doping of the M-derived states shows a decrease in intensity, but no shift, either a crossover towards a truly metallic Fermi level. The M d spectral weight is peaked at  $0.3E$  eV below  $E_F$ . Note that in a real impurity system, i.e., where disorder is included, Bloch states are never formed and the concept of delocalized states in the M-derived band with a clear  $E$  vs.  $k$  relation cannot be fully defined. Thus the term band does not imply electronic states of well-defined crystal momentum, while the  $1/3S$  represents a well-defined quantity. In the present case, a  $6eV$  resolution  $\epsilon$  measures only the  $1/3S$  due to the high photoenergy used  $=h\nu \approx 5.4eV$ , band structure effects can be neglected B1, C.

Knowing that the key differences between the  $\epsilon$  band and the impurity band model are found in the description of the nature of the electronic wave functions immediately adjacent to  $E_F$  with respect to the  $\epsilon$  band states,



the presence of electrical observations of a persistent diluted character of M- ions, together with the related effects on the system, as reported by Shyba *et al.* It is suggested that the existence of a M- derivative band which is not detected for the ions bands, could be compatible at the same time with the relative purity band character.

On the other hand, our preliminary results provide experimental and theoretical evidence of a persistent diluted character of M- ions, up to high concentrations. The presence and importance of electrostatic correlations in the vicinity of the Fermi level, and at the same time the fundamental role of the delocalized M- derivative electrostates for the ferroelectric character of the system.

### Acknowledgements

The authors are gratefully acknowledged the support of the US Department of Energy under contract No. DE-AC02-81OR21400. Financial support for the present work is provided by the Austrian Science Foundation SFB (SFB 154/23 and 154/24), the Austrian Ministry of Science and Research (BMBWF) and the Austrian Research Federation (FFG) project 8155. The authors are also grateful to J.M., J.B., ... and #.\$. 0.1.M. and 3./ are grateful to the Swedish Research Council (KR), the German-Dutch cooperation (S/M), the K. Foundation and the R&E (S1). The authors are also grateful to the M. O. Katselso for useful discussions.

### REFERENCES

9pa-a22io-e6Uelettra.trieste.it

10 ) . . . Ma2do-ald, #. S2hi??er a-d F. Sa ! arth, Future Mater. **4**, 1, 5 (2005).

B2C O. Vutić, J. Fabian and S. Las Saraja, *Rev. Mod. Phys.* **76**, 323 (2004).

B3C G. Knap, J. Fert and F. Fegyveresi-Kaufmann, *Future Mater.* **6**, (13 (2018)).

B4C F. Saraj, *Future Mater.* **11**, 3 (2018).

B5C S. Ietl, *Future Mater.* **9**, (5 (2017)).

B6C S. Jung, J. Siy, J. Maier, J. Kuehner and ... Maitland, *Rev. Mod. Phys.* **78**, (E, (2006)).

B7C S. Ietl, ... Shio, F. Matsuzura, J. Kibert, I. Ferrer, S. Ietl **287**, 1E1, (2006).

B8C S. Shio, K. Saita and M. Saita, *Future Phys.* **7**, 342 (2011).

B9C J. Masera, J. et al., *Phys. Rev. Lett.* **105**, 22 (2010).

B10C K. Sato et al., *Rev. Mod. Phys.* **82**, 1 (2010).

B11C ). \*. +ray et al., *Fat. Mater.* **11**, (5 (2012)).

B12C O. Li Marzo, O. . et al., arXiv:1201.2012 (2012).

B13C ). Riethardella et al., *S. Ietl* **327**, (5 (2010)).

B14C J. S. Abayashi et al., *Phys. Rev. B* **64**, 1253E4 (2001).

B15C J. S. Abayashi et al., *Phys. Rev. B* **58**, R4211 (1998).

B16C M. Saito et al., *Future Phys.* **6**, 22 (2010).

B17C +. #a-a2io-e and K. Kobayashi, *Surf. Science* **606**, 125 (2012).

B18C ). \*. +ray et al., *Future Mater.* **10**, (5 (2011)).

B19C See Supplemental Material for detailed information on the sample preparation, the calibration and the details of the calculations.

B20C J. Miyazaki, *J. Phys. Chem. C* **23**, 2532E1 (2011).

B21C ... /bert et al., *Rep. Prog. Phys.* **74**, E (2011).

B22C #. Shustrova, #. et al., *Phys. Rev. Lett.* **109**, 1 (2012).

B23C +. Kotliar et al., *Rev. Mod. Phys.* **78**, (5 (2006)).

B24C J. Braun et al., *Phys. Rev. B* **82**, E24411 (2010).

B25C J. Fujii et al., *Phys. Rev. Lett.* **107**, 1 (2011).

B26C K. ... /dots et al., *Phys. Rev. Lett.* **107**, 1, (2011).

B27C M. Iobrools et al., *Future Mater.* **11**, 444 (2018).

B28C S. Kim et al., *Phys. Rev. B* **310**, (3 (2014)).

B29C +. Kaderbas et al., *Phys. Rev. B* **81**, 214422 (2010).

## FIGURE CAPTIONS

**FIG. 1.** (Color online) (a-c) HAXPES spectra ( $h\nu = 5953$  eV) for different Mn doping in GaAs. For the sake of comparison, the GaAs spectra have been aligned to the (GaMn)As

spectra using the BE position of the As 4s core level. No background subtraction was applied. **(a)** Extended valence band PES ( $T = 20$  K), including the As 4s, Ga 4s, and As 4p shallow core levels of GaAs(100) and 13% Mn doped GaAs. **(b)** Zoom of the valence band region ( $T = 100$  K), showing the spectra from pure GaAs (black dots), 1% and 13% Mn doped GaAs (red and blue dots, respectively). **(c)** High-resolution spectra measured in the vicinity of  $E_F$ . Difference spectra, corresponding to the Mn contribution only, are shown in orange [13% Mn spectrum (blue dots) minus pure GaAs spectrum (black dots)] and grey [1% Mn spectrum (red dots) minus pure GaAs spectrum (black dots)]. **(d)** Calculated angle-integrated PES (including matrix elements) for photon energy and geometry ( $p$ -polarization) as used in the experiment. **(e)** Calculated valence-band spectra of GaAs(100) using LDA (black curve) and (Ga,Mn)As (13%) using both LDA (red curve) and DMFT (blue curve). **(f)** Zoom of the vicinity of  $E_F$  with calculated difference spectra, as in panel **(c)**, for LDA (violet curve) and DMFT (green curve).

**FIG. 2.** (Color online) **(a)** HAXPES wide energy scan ( $h\nu = 7940$  eV, linear polarization,  $T = 20$  K) of 13% Mn doped GaAs. Main lines positions are indicated. The inset shows a zoom of the Mn 2p core level with the  $2p_{1/2}$  and  $2p_{3/2}$  multiplet structure, where the well-screened and poorly-screened peaks are indicated. For an explicit definition of well and poor screened peaks in (GaMn)As see ref [25]. **(b)** Magnetic circular dichroism (MCD) in HAXPES. Polarization dependent Mn 2p spectra (blue and red dots for right- and left-circular polarization, respectively), measured at  $T = 20$  K, i.e., in the ferromagnetic state below  $T_C$ ; the dashed thin line represents the background. In the lower panel the difference spectrum (MCD), representing the magnetic signal (open white circles) is shown; the green line is a smoothed curve. The value of the maximum magnetic asymmetry, defined as  $(I^+ - I^-)/(I^+ + I^-)$ , where  $I^+$  ( $I^-$ ) is the intensity measured with Circ+ (Circ-), is indicated. **(c)** Calculations for a hybridization  $V$ , as well as a fully localized  $d^5$  state, and iterative electronic structure calculations.

calculated curves are offset for clarity. The best agreement is for a hybridization parameter  $2.0 \leq V \leq 2.5$  eV.

**FIG. 3.** (Color online) Temperature dependence of the (Ga,Mn)As (13% Mn) PES. **(a)** Relative BE shift of the GaAs host valence band, Ga  $2p$  core level, Mn  $2p_{3/2}$  low energy feature, and Mn  $2p_{3/2}$  broad peak; the BEs at 20 K are used as reference. **(b)** Mn  $2p_{3/2}$  core level measured at 20 K and at RT.

**FIG. 4.** (Color online) Schematics summarizing our conclusions regarding the electronic structure of (Ga,Mn)As. **(a)** Experimental valence band (smoothed) at  $h\nu = 5953$  eV. GaAs host band (blue curve) and (Ga,Mn)As band with 13% Mn (red curve). The difference between both spectra identifies the Mn-derived states (dark green). The dashed vertical bar marks the position of  $E_F$ ; the center of the Mn band is located at 300 meV BE. **(b)** The bottom panel shows a zoom of the region near  $E_F$ . The GaAs host band does not cross  $E_F$  (energy separation of 50 meV) but the Mn-induced states have a finite non-zero density at  $E_F$ . The color shading illustrates the difference in electronic character of the Mn  $d$ -states as derived from our theoretical calculations: near  $E_F$  a  $3d^5h$  localized character is found, whereas  $3d^6h^2$  delocalized character is assigned to the dark green region. The latter corresponds to the hybridization responsible for mediating the ferromagnetism.

Fig. 1

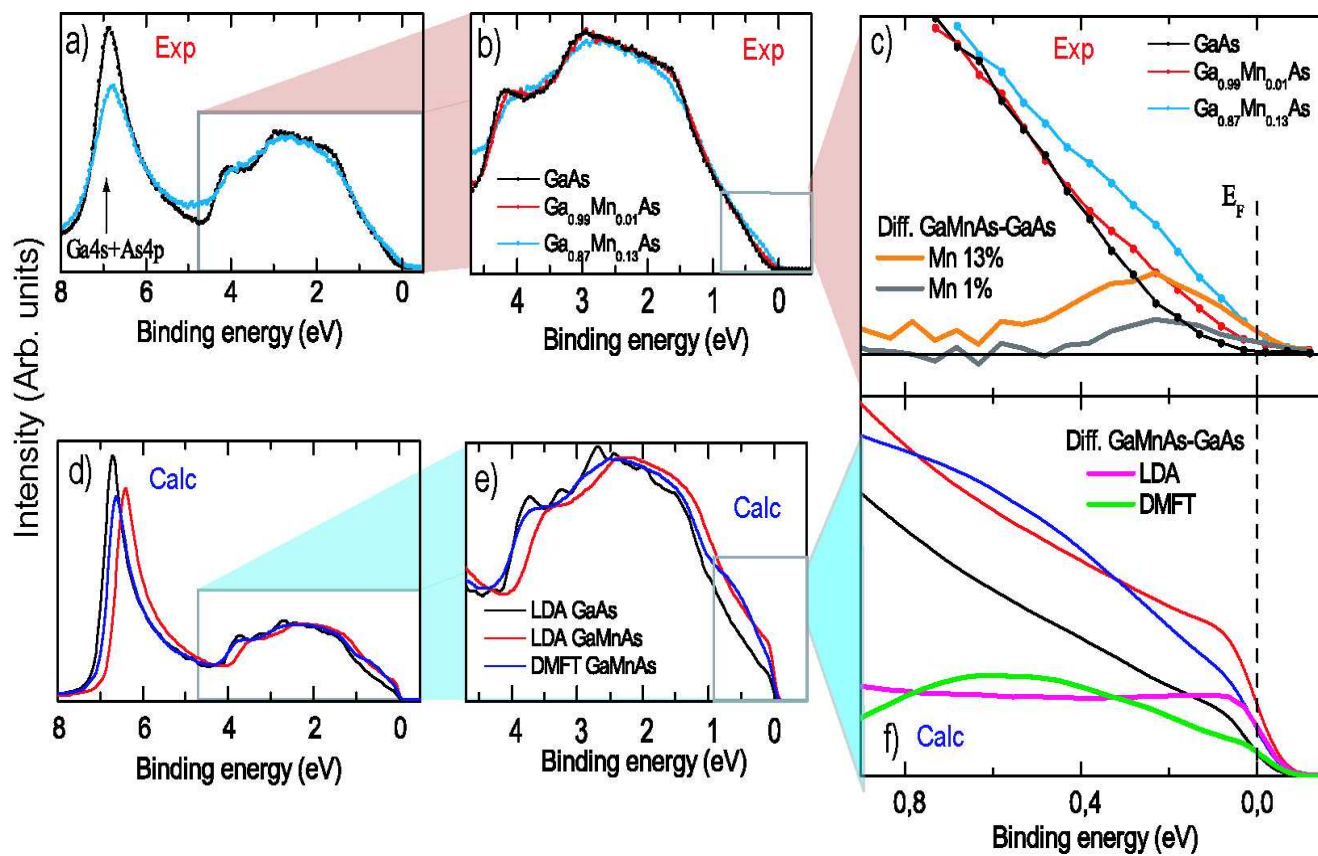


**Fig. 2**

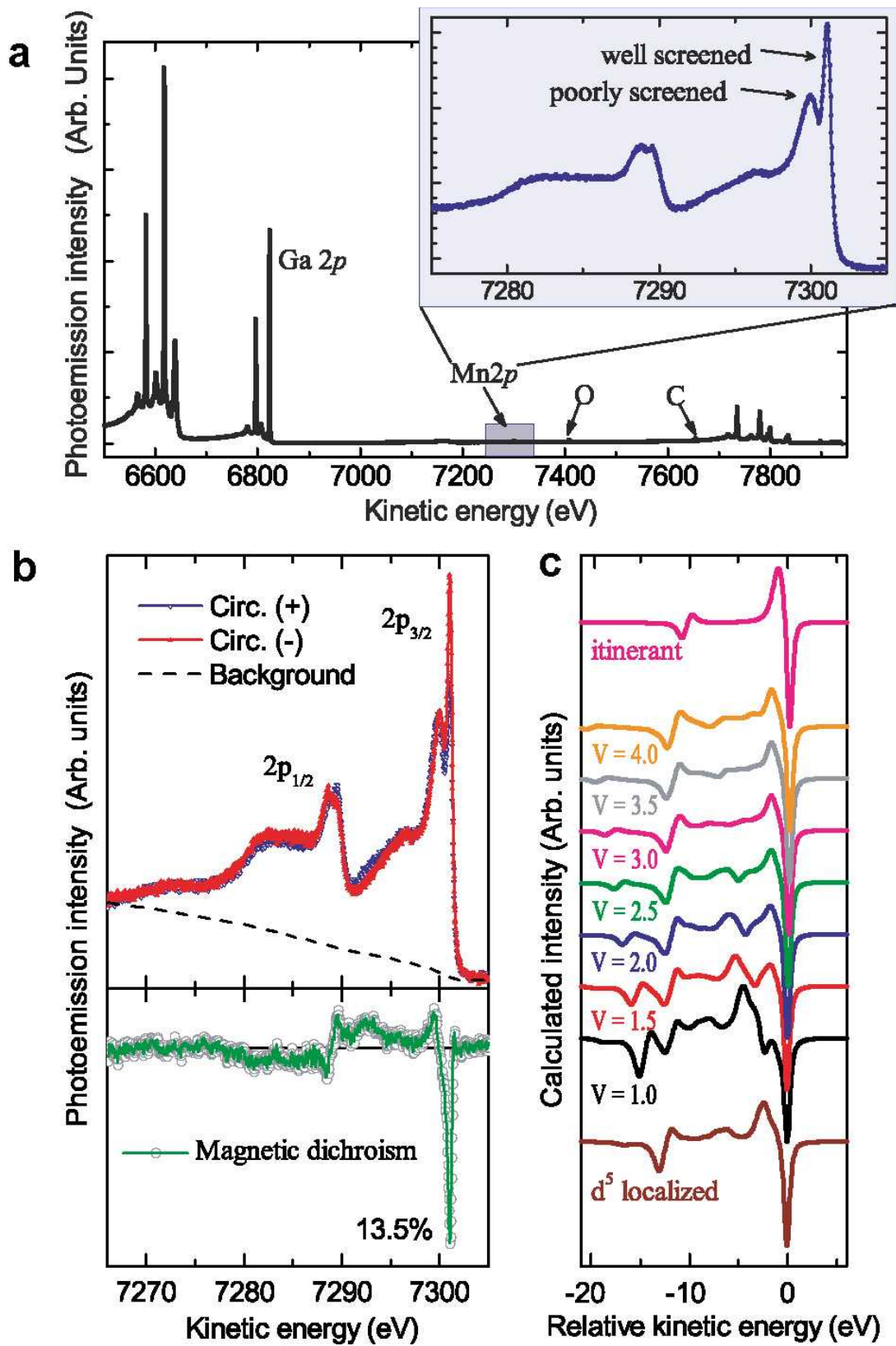


Fig. 3

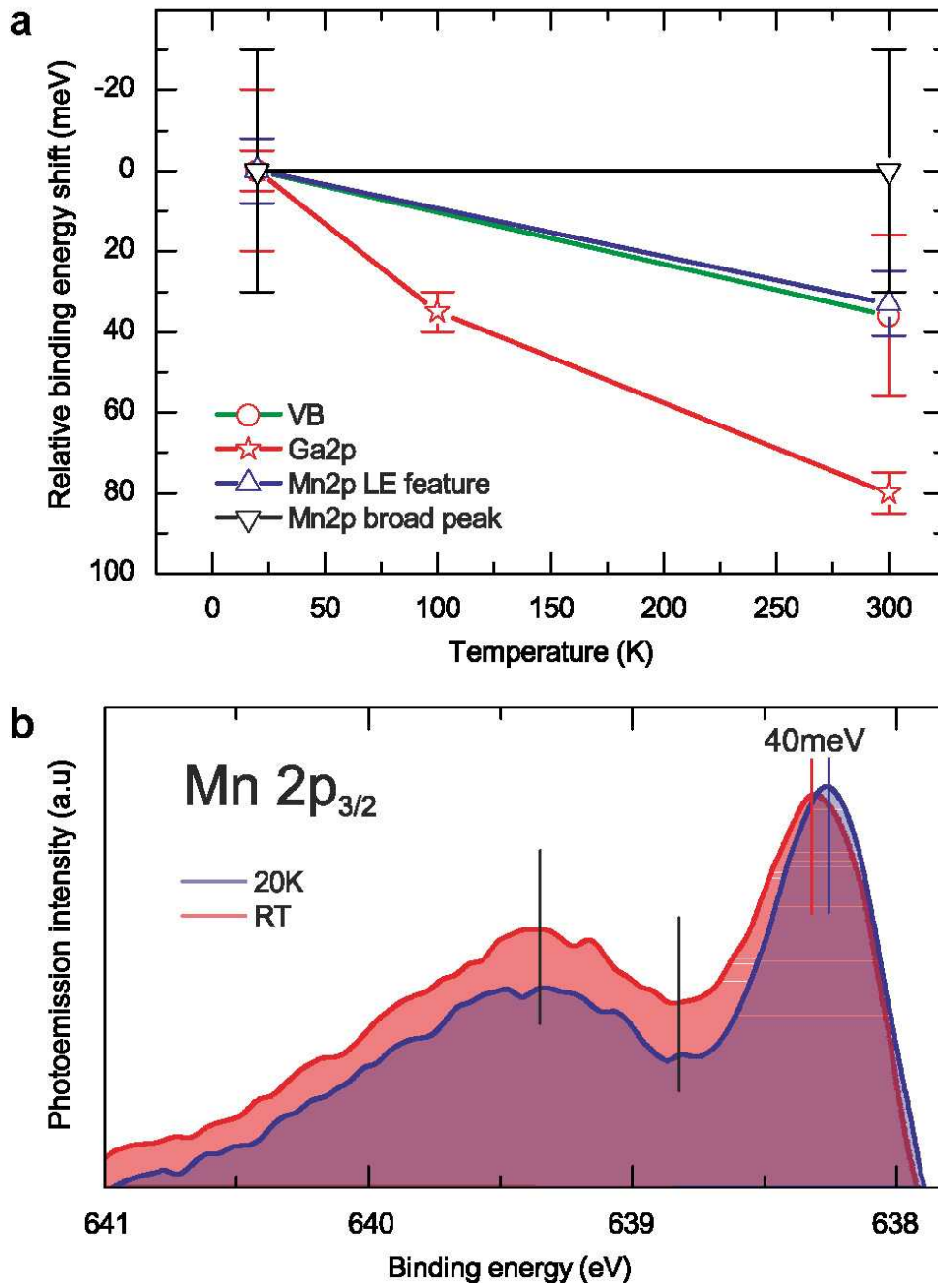


Fig. 4



